



Voltammetric and thermodynamic studies of the $\text{VOSO}_4 \cdot 5\text{H}_2\text{O}$ and N-3-phenylallylidene nicotinohydrazide complexation system

Alaa S. Nageeb*, Mohamed A. Morsi, Esam A. Gomaa, Mohamed M. Hammouda, Rania R. Zaky

Chemistry Department, Faculty of Science, Mansoura University, Mansoura, Egypt

* Correspondence to: alaa_saleh715@yahoo.com, 01097730418

Received: 2/1/2024
Accepted: 18/1/2024

Abstract: A multichannel potentiostat of the type DY2100 was used to conduct a comprehensive thermodynamic/kinetic study on the redox activity of the VO(II) cation in the absence and presence of the synthesized N-3-phenylallylidene nicotinohydrazide HNP ligand. The cyclic voltammetry experiment was operated at a glassy carbon electrode surface as a working electrode and at a room temperature of 305°K. NaClO_4 sodium perchlorate solution with a concentration of 0.1 M was prepared to act as an electrolytic medium. Various kinetic/thermodynamic parameters were provided, which exhibited a linear increase with increasing VO(II) concentration. The reaction mechanism was suggested depending on Nicholson's theory, whereas the VO(II) ion's redox activity in the absence and presence of HNP underwent a reversible chemical reaction preceding a reversible electron transfer mechanism. Furthermore, the thermodynamic characteristics expressed in Gipps free energy and the stability constant of the complexation process were assessed. After the end of the addition of the HNP, the Gipps free energy and the stability constant were estimated to be -19.5 kJ and 2264.13, respectively, and these findings revealed that the process occurred spontaneously

keywords: Cyclic voltammetry, Gipps free energy, Formation constant

1. Introduction

Vanadium ion spreads naturally as a trace element in the soil, water, and different biological systems in the environment. Typically, vanadium ions exist in the form of oxides, carrying different oxidation states III, IV, and V. However, these oxides play the role of the metal cations. Among these common oxides are vanadyl sulfate VOSO_4 and sodium metavanadate NaVO_3 , which can act as insulin mimetic agents [1-4]. Particularly, vanadium ions can be concentrated to higher concentrations because they can be strongly complexed with numerous organic ligands. This method succeeded in pre-concentrating of vanadium ions in lakes, rivers, and oceans. According to these facts, it is convenient to use appropriate analytical methods such as cyclic voltammetry to detect VO(II) in the environment. It is also appropriate to take advantage of its ability to form multi-metallic complexes with different ligands to do several studies and applications [5-7]. Cyclic voltammetry was first employed by Randless in

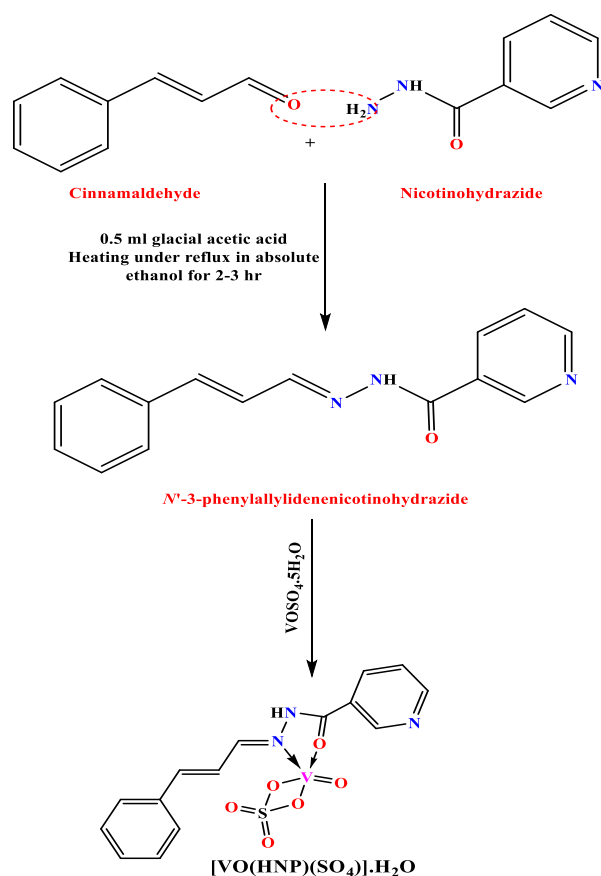
1938 and occupied great important among other analytical strategies. Cyclic voltammetry enables the oxidation and reduction of different organic and inorganic substances if the appropriate energy is provided. Herein, the redox activity of the VO(II) cation either in the absence or presence of the HNP was investigated at the surface of the glassy carbon electrode, applying a potential difference ranging from -0.8 to 1.2 V. Various kinetic and thermodynamic parameters were evaluated such as k_s (rate of charge transfer), Γ_c (surface concentration during anodic reaction), Γ_a (surface concentration during cathodic reaction), Q_c (charge quantity estimated during cathodic process), and Q_a (charge quantity estimated during anodic process). Moreover, the Nicholson theory and Randless equation were applied to suggest the reaction mechanism [8-9].

2. Materials and methods

The used chemicals in this research were $\text{VO}(\text{SO}_4)_2 \cdot 5\text{H}_2\text{O}$, NaClO_4 , nicotinohydrazide, cinnamaldehyde, and absolute ethanol. These chemicals were obtained from Sigma Aldrich Company and were used without any purification.

2.1 preparation of HNP ligand

The preparation of HNP ligand is described in scheme 1. The method of preparation and characterization was reported by Nageeb, Alaa S., et al. [10].



Scheme 1: The outline strategy of the HNP preparation and its VO(II) complex

2.2. Cyclic voltammetry measurements

A three electrode electrochemical cell with a 50-ml cell volume was connected to a multichannel potentiostat. The used electrodes were of the type glassy carbon with an area of 0.07 cm^2 as the working electrode, $\text{Ag}/\text{AgCl}/\text{KCl}$ sat. as the reference electrode, and platinum wire as the counter electrode. The employed electrodes were immersed in a 50 ml of NaClO_4 solution with a concentration of 0.1 M, acting as an electrolytic media. The cyclic voltammetry scanning was operated at 305°K and a potential range of -0.8 to 1.2 V . To

remove any dissolved oxygen, nitrogen gas was passed through the solution before each measurement [11-12].

3. Results and Discussion

3.1. The employed equation in the kinetic thermodynamic study

The redox system of the VO/VO^{2+} couple was studied by applying several equations as follows:

$$\Delta E_p = E_{p_a} - E_{p_c} \quad (1)$$

$$E_{1/2} = (E_{p_a} + E_{p_c})/2 \quad (2)$$

Where, E_{p_a} refers to the anodic peak potential, E_{p_c} refers to the cathodic peak potential, ΔE_p refers to the difference between anodic and cathodic potential, and $E_{1/2}$ refers to the half wave potential.

$$I_p = 0.4463 nFA C (nFvD/RT)^{1/2} \quad (3)$$

$$\Gamma = I_p 4RT/n^2 F^2 Av \quad (4)$$

$$K_s =$$

$$2.18 (Dc \text{ ana } Fv/RT)^{1/2} \exp(\alpha^2 nF(E_{p_c} - E_{p_a})/RT) \quad (5)$$

$$Q = nFA\Gamma \quad (6)$$

Where, I_p refers to the current peak (ampere), I_{p_a} refers to the anodic peak current, I_{p_c} refers to the cathodic peak current, R refers to the gas constant and equals 8.314 J/mol.K , n refers to the number of electrons involved in the redox process, T refers to the temperature in kelvin, v is the applied scan rate in V/s , C refers to the concentration of the electroactive species in mol/cm^3 , F refers to faraday constant and equals 96485 C/mol , A refers to the electrode area in cm^2 , Γ refers to the surface concentration in mol/cm^2 , k_s refers to the heterogeneous charge transfer rate constant in cm/s , α refers to the charge transfer parameter, which is regarded as 0.5 for a quasi-reversible reaction, and Q is the amount of electricity that was consumed during the redox process in coulomb.

$$\Delta E_{1/2} = (E_{1/2})_C - (E_{1/2})_M = 2.303 \frac{RT}{nF} (\text{Log } \beta_c + j \text{Log } C_L) \quad (7)$$

$$\Delta G = -2.303 RT \text{Log } \beta_c \quad (8)$$

Where, β_c refers to the stability constant for the complex formation, $(E_{1/2})_M$ refers to the half wave potential of the metal cation. Upon the final addition, $(E_{1/2})_C$ refers to the half wave

potential of the complexation upon each addition of the HNP, and ΔG refers to the Gibbs free energy of the complexation reaction [13-20].

3.2. Cyclic voltammetry of VO(II) ion

On applying cyclic voltammetry of 19.6×10^{-4} M $\text{VOSO}_4 \cdot 5\text{H}_2\text{O}$, it was observed that one cathodic peak appeared ~ 0.18 V referred to the $\text{VO}^{2+} + 2e \rightarrow \text{VO}$ and one anodic peak appeared at approximately 1.12 V referred to as the $\text{VO} \rightarrow \text{VO}^{2+} + 2e$ reaction, as depicted in Fig. 1. As a result, a quasi-reversible reaction mechanism was proposed for the VO/VO(II) redox couple.

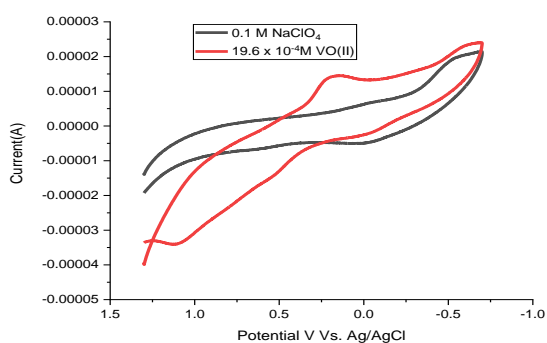


Fig.1: Cyclic voltammogram of 19.6×10^{-4} M $\text{VOSO}_4 \cdot 5\text{H}_2\text{O}$ in a 0.1 M NaClO_4 as supporting electrolyte.

3.2.1 The impact of increasing VO(II) concentrations on the kinetic parameters

$(3.9, 7.9, 11.8, 15.7, 19.6) \times 10^{-4}$ M were employed as various concentrations of the VO(II) ion to study the impact of increasing

Table 1: The impact of increasing concentration of the VO(II) ion on the evaluated kinetic parameters.

$[\text{VO}^{2+}] \times 10^{-4}$ mol/L	$\text{Ipa} \times 10^{-6}$ (A)	$\text{Ipc} \times 10^{-6}$ (A)	Ipa/Ipc (A)	Epa (V)	Epc (V)	ΔE (V)	$\text{E}_{1/2}$ (V)	$\text{Da} \times 10^{-13}$ cm^2/s	$\text{Dc} \times 10^{-14}$ cm^2/s	$\Gamma_a \times 10^{-10}$ mol/ cm^2	$\Gamma_c \times 10^{-10}$ mol/ cm^2	$\text{Qa} \times 10^{-6}$ (C)	$\text{Qc} \times 10^{-6}$ (C)	$\text{Ks} \times 10^2$ cm/s
3.98	3.3	1.1	3.06	0.531	0.0003	0.531	0.265	2.5	2.7	5.2	0.42	3.5	0.57	0.95
7.94	4.4	3.4	1.27	0.827	0.191	0.635	0.509	1.1	6.7	6.8	1.3	4.6	1.8	0.43
11.86	5.7	4.7	1.21	0.715	0.172	0.543	0.444	0.83	5.7	8.8	1.8	5.9	2.4	0.07
15.75	6.9	6.5	1.05	1.074	0.182	0.891	0.628	0.69	6.2	10.7	2.5	7.2	3.4	56
19.6	10.4	8.04	1.29	1.098	0.191	0.906	0.644	8.1	6.1	16.1	3.1	10.9	4.2	70

concentration on the current, kinetic parameter, and reaction mechanism. Upon increasing VO(II) concentration, both the cathodic and anodic current exhibited a gradual increase, as depicted in Fig. 2,3. According to Randles Sevcik equation Eq.3, a linear plot of peak current against the employed con.

centrations was obtained. So, a diffusion controlled mechanism was suggested for the $\text{VO} \rightarrow \text{VO}^{2+} + 2e$ reaction. The kinetic parameters, including Γ_c , Qc , Γ_a and Qa , as listed in Table 1, increased linearly with the increase in current. In addition, both Da and Dc increases with the progress of the oxidation reduction reaction. The peak current ratio doesn't equal unity, indicating a quasi-reversible process. The rate of electron transfer increased with the increase in concentration, favoring the charge transfer process [21].

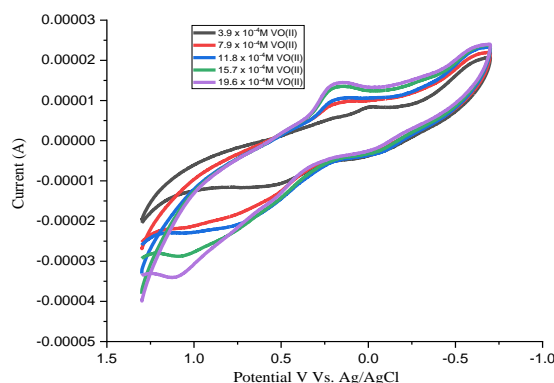


Fig.2: Cyclic voltammogram of various concentrations of $\text{VOSO}_4 \cdot 5\text{H}_2\text{O}$ in a 0.1 M NaClO_4 as supporting electrolyte

Table 2: The impact of employing different scan rates on the evaluated kinetic parameters

$[\text{VO}^{2+}] \times 10^{-4}$ mol/L	Sc V/s	$(-)\text{Ipa} \times 10^{-6}$ (A)	$\text{Ipc} \times 10^{-6}$ (A)	Ipa/Ipc (A)	Epa (V)	Epc (V)	$\text{Da} \times 10^{-13}$ cm^2/s	$\text{Dc} \times 10^{-14}$ cm^2/s	$\Gamma_a \times 10^{-10}$ mol/ cm^2	$\Gamma_c \times 10^{-10}$ mol/ cm^2	$\text{Qa} \times 10^{-6}$ (C)	$\text{Qc} \times 10^{-6}$ (C)	Ks cm/s
19.6	0.1	10.4	8.04	1.29	1.09	0.19	1.02	6.08	4.04	3.12	5.4	8.4	7006.92
19.6	0.05	4.0	6.5	0.60	1.05	0.21	0.3	8.17	3.11	5.12	4.2	13.8	1361.54
19.6	0.02	3.6	4.2	0.86	1.04	0.23	0.6	8.33	7.08	8.19	9.5	22.1	530.58
19.6	0.01	0.1	3.4	0.02	0.68	0.21	0.0094	11.1	0.38	1.33	0.52	36.05	0.78

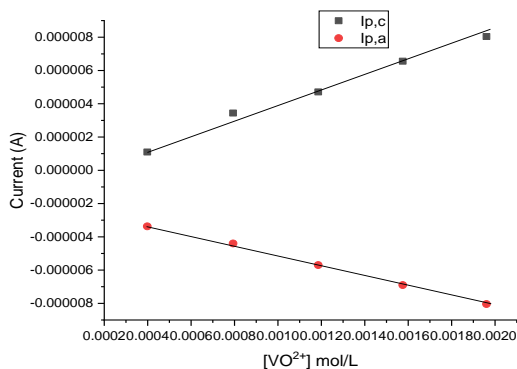


Fig.3: The plot of peak current versus different concentrations of $\text{VOSO}_4 \cdot 5\text{H}_2\text{O}$

3.2.2 The impact of applying diverse scan rate

Randles Sevcik equation Eq.3 allows studying the relation between the peak current and the square root of the scan rate. The linear relationship between the peak current and the

square root of the scan rate is indicative of the diffusion controlled mechanism. Different scan

rates 0.01, 0.02, 0.05, and 0.1 V/s were applied to study the mechanism of the redox reaction, as depicted in Fig. 4. The plot of I_p versus $v^{1/2}$ yielded a straight line, suggesting a diffusion controlled mechanism, as depicted in Fig. 5. Furthermore, all evaluated kinetic parameters, including k_s , Γ_c , Q_c , Γ_a , and Q_a were influenced by applying different scan rates.

The scan rate is typically related to the volt quantity consumed per time; thus, altering the reaction scan rate causes altering of the current response. The decrease of the scan rate from 0.1 to 0.01 V/s causes a decrease in the observed current, which reflects the rate of the oxidation and reduction processes occurring at the electrode surface. This means that the decreasing in the scan rate causes a decrease in the rate of charge transfer that is responsible for the progress of the oxidation reduction reaction and vice versa, accordingly, the value of k_s decreases. The other kinetic parameters Γ_c , Q_c , Γ_a , and Q_a , which depends mainly on the current response, as described in Eq. 4,6, decreased due to the decrease in current [22], as listed in Table 2.

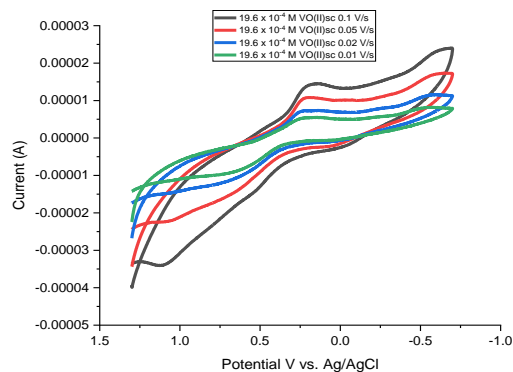


Fig.4: Cyclic voltammogram of various scan rates of $19.6 \times 10^{-4} \text{ M VOSO}_4 \cdot 5\text{H}_2\text{O}$ in a 0.1 M NaClO_4 as supporting electrolyte.

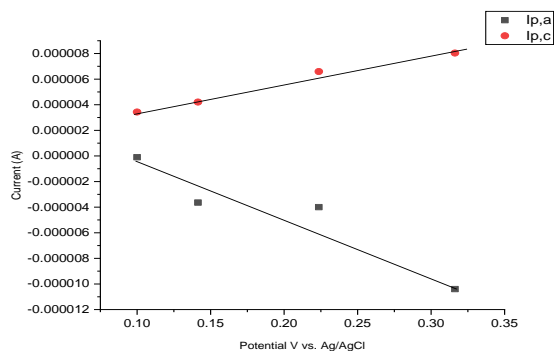


Fig.5: The plot of I_p against square root of a $19.6 \times 10^{-4} \text{ M VOSO}_4 \cdot 5\text{H}_2\text{O}$ in a 0.1 M NaClO_4

3.2.3 Suggestion of reaction mechanism

The redox reaction mechanism of $\text{VOSO}_4 \cdot \text{H}_2\text{O}$ on the glassy carbon electrode surface can be proposed with the aid of Nicholson theory,

which involves different hypotheses of reaction mechanisms, as shown in Fig.6. These hypotheses can be applied depending on the relation between peak current ratio and scan rate, as illustrated in Fig.7. The plot of peak current ratio versus scan rate of the redox reaction $\text{VO} \rightarrow \text{VO}^{2+} + 2e$ yielded a relationship, predicting that this reaction is a reversible chemical reaction preceding a reversible electron transfer, following this general equation $\text{O} + ne \rightleftharpoons \text{R}$. [23]

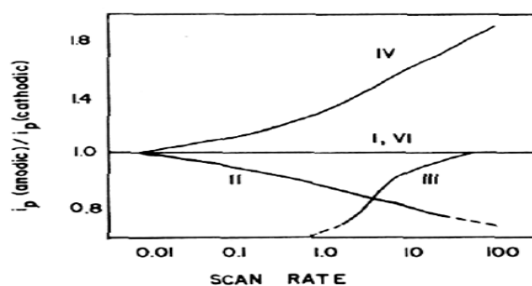


Fig. 6: The standard plot of Nicholson theory

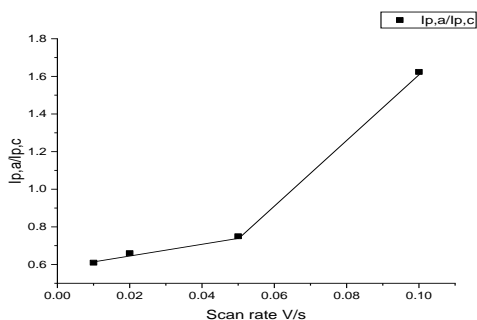


Fig.7: The plot of peak current ratio versus scan rate

3.3 The impact of the addition of HNP ligand on the redox behavior of VO(II) cation

The redox activity of the VO(II) cation was investigated in the presence of HNP ligand. Upon the addition of 1.9×10^{-4} M of HNP ligand to 19.4×10^{-4} M of VO(II) ion, the cyclic voltammogram showed a strong decrease in peak current intensity, either the cathodic or the anodic, and a shift of the peak potential to new positions. This can be interpreted due to the strong and stable complexation reaction between the VO(II) and HNP, as depicted in Fig. 8.

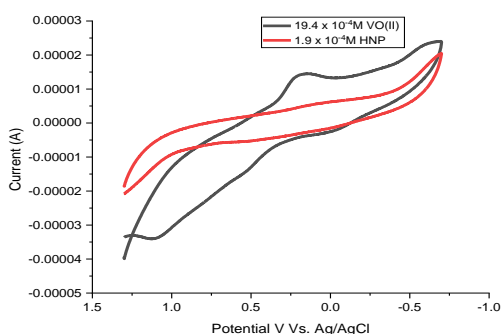


Fig. 8: The impact of addition of a 1.9×10^{-4} M of HNP to a 19.4×10^{-4} M VO(II) ion

3.3.1.impact of various concentrations of HNP on the kinetic parameters

$(3.7, 7.2, 10.5, 13.5, \text{ and } 16.3) \times 10^{-4}$ M were employed as various concentrations of the HNP to study its complexation effect on the VO(II) ion. It was observed that both cathodic and anodic currents exhibited a linear decrease with the addition of HNP, indicating a decrease in the VO(II) ion concentration due to the complexation process, as shown in Fig. 9,10. According to the complex formation, all evaluated kinetic parameters and the rate of electron transfer decreased [24], as listed in Table 3.

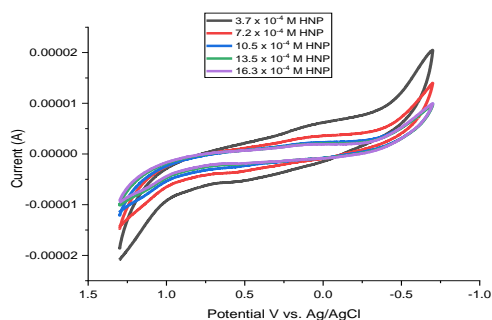


Fig.9: The impact of increasing concentration of HNP on the redox behavior of the VO(II) ion.

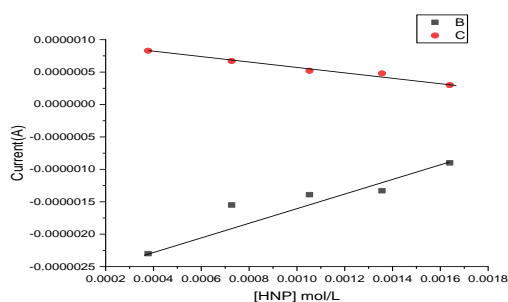


Fig.10: The plot of peak current versus different concentrations of HNP

3.3.2.The impact of applying diverse scan rate

Different scan rates 0.01, 0.04, 0.02, and 0.01V/s were employed to study the complexation reaction between a 16.3×10^{-4} M HNP with a 19.3×10^{-4} M VO(II) within the solution, as shown in Fig.11. It was concluded that both cathodic and anodic peak current as well as the peak potential separation decreased, indicating a quasi-reversible complexation reaction. Meanwhile, the plot of peak current versus square root of scan rate yielded a straight line, unveiling that the reaction was diffusion controlled, as shown in Fig.12. All evaluated kinetic parameters decreased as a result of complexation process, as listed in Table 4

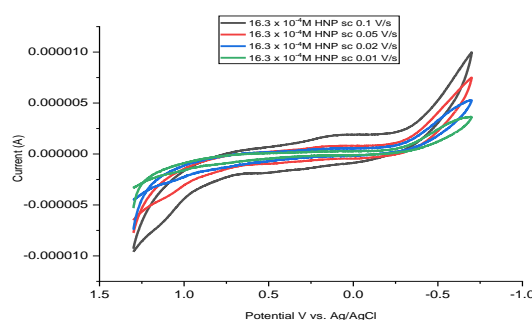


Fig.11: Cyclic voltammogram of various scan at final addition of HNP ligand

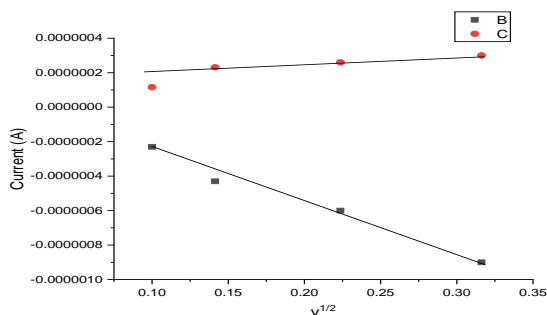


Fig.12: The plot of I_p against square root of at final addition of HNP.

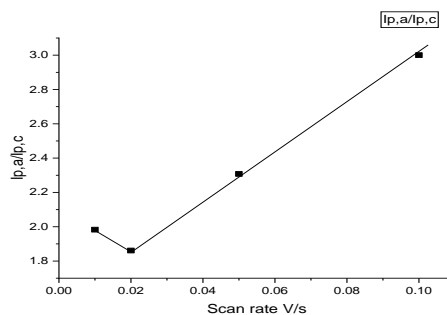


Fig.13: The plot of peak current ratio versus scan rate

3.3 Suggestion of reaction mechanism

According to Nicholson theory, the mechanism of complexation reaction can be suggested. A plot of peak current ratio against scan rate was performed to propose the mechanism of complexation related to the hypotheses of Nicholson theory, as shown in Fig.13. Accordingly, it was concluded that the complexation between the HNP and VO(II) followed a reversible chemical reaction preceding a reversible electron transfer mechanism, referring to this general equation $O + ne \rightleftharpoons R$.

3.4 The investigation of the reaction spontaneity

Typically, Gibbs free energy is very important parameter from the thermodynamic point of view. This parameter usually evaluates the spontaneity of the process according to its negative value. Lingane equation Eq.7 was applied to estimate the stability constant of complex formation. Afterward, Eq.8 was applied to estimate Gibbs free energy of the process, as listed in Table 4. Hence, the spontaneity of the reaction can be concluded from the calculated stability constant and the negative value of the Gibbs free energy [25].

Table 3: The impact of increasing concentration of the HNP on the evaluated kinetic parameters.

[HNP] $\times 10^{-4}$ mol/L	$I_{pa} \times 10^{-6}$ (A)	$I_{pc} \times 10^{-7}$ (A)	I_{pa}/I_{pc} (A)	E_{pa} (V)	E_{pc} (V)	ΔE (V)	$E_{1/2}$ (V)	$D_a \times 10^{-15}$ cm^2/s	$D_c \times 10^{-16}$ cm^2/s	$\Gamma_a \times 10^{-10}$ mol/cm ²	$\Gamma_c \times 10^{-11}$ mol/cm ²	$Q_a \times 10^{-6}$ (C)	$Q_c \times 10^{-7}$ (C)	$K_s \times 10^2$ cm/s
3.7	2.3	8.3	2.7	1.21	0.08	1.13	0.64	4.9	6.4	3.5	3.2	2.4	4.3	90
7.2	1.5	6.7	2.3	1.15	0.10	1.05	0.62	2.2	4.2	2.4	2.6	1.6	3.5	13
10.5	1.39	5.2	2.6	1.13	0.08	1.05	0.60	1.8	2.5	2.1	2.02	1.4	2.7	11
13.5	1.3	4.8	2.7	1.10	0.10	1.00	0.60	1.6	2.1	2.07	1.8	1.3	2.5	40
16.3	0.9	3.0	3.0	1.11	0.11	0.99	0.61	0.7	0.8	1.4	1.1	0.9	1.5	20

Table 4: The impact of employing different scan rates on the evaluated kinetic parameters.

[HNP] $\times 10^{-4}$ mol/L	Sc V/s	$(-I_{pa}) \times 10^{-7}$ (A)	$I_{pc} \times 10^{-7}$ (A)	I_{pa}/I_{pc} (A)	E_{pa} (V)	E_{pc} (V)	ΔE (V)	$D_a \times 10^{-15}$ cm^2/s	$D_c \times 10^{-4}$ cm^2/s	$\Gamma_a \times 10^{-10}$ mol/cm ²	$\Gamma_c \times 10^{-5}$ mol/cm ²	$Q_a \times 10^{-6}$ (C)	Q_c (C)	K_s cm/s
16.3	0.1	9.0	3.0	3	1.1	0.11	0.99	6.09	11.6	1.4	4.3	94.6	0.58	13.7
16.3	0.05	6.0	2.6	2.3	1.08	0.14	0.94	5.42	22.3	1.8	8.4	1.26	1.14	8.6
16.3	0.02	4.3	2.3	1.8	1.07	0.14	0.93	6.96	54.7	3.3	20.9	2.26	2.8	8.5
16.3	0.01	2.3	1.1	1.9	1.05	0.15	0.90	3.98	10.4	3.5	41.05	2.41	5.54	7.7

Table 4: The concluded β_c and ΔG (kJ) of the complexation process between the VO(II) cation and HNP.

[HNP] $\times 10^{-4}$ mol/L	$[VO^{2+}] \times 10^{-4}$ mol/L	j [M/L]	$E_{1/2(c)}$ V	$E_{1/2(M)}$ V	$\Delta E_{1/2}$ V	β_c	ΔG (kJ)
3.7	19.6	0.19	0.64	0.64	0.002	5.67	-4.4
7.2	19.6	0.36	0.62	0.64	0.018	60.94	-10.4
10.5	19.6	0.53	0.60	0.64	0.038	737.25	-16.7
13.5	19.6	0.68	0.60	0.64	0.038	1790.28	-18.9
16.3	19.6	0.83	0.61	0.64	0.031	2264.13	-19.5

4. Conclusion

In summary, Cyclic voltammetry technique was applied as an appropriate method to study the redox behavior of the VO(II) ion and its ability to complex with the prepared ligand HNP in solution. At the end of the study, it was possible to obtain several conclusions. The VO(II), in the form of $\text{VOSO}_4 \cdot 5\text{H}_2\text{O}$, is an

electroactive species, which underwent

oxidation and reduction reaction at glassy carbon electrode surface, following these redox equations: $\text{VO}^{2+} + 2e \rightarrow \text{VO}$



The electrochemical behavior of VO(II) cation exhibited one cathodic peak and one anodic peak, recording peak current ratio $\neq 1$ and small ΔE , indicating a quasi-reversible reaction. According to Nicholson theory assumptions, the reaction mechanism was proposed to be a reversible chemical reaction preceding a reversible electron transfer. The peak current ratio I_{pa}/I_{pc} recorded during the reaction of the VO(II) and HNP $\neq 1$. Furthermore, the peak potential separation ΔE is small value, implying that the complexation reaction was a quasi-reversible. Based on Randles equation Eq. 3, it was found that the the VO(II) ion's redox activity in absence and presence of HNP was governed by diffusion. The reaction between the VO(II) and HNP occurred spontaneously, which can be indicated from the calculated stability constant and negative Gibbs free energy. Nicholson theory also revealed that the complexation

reaction followed a reversible chemical reaction mechanism preceding a reversible electron transfer.

References

- 1 Mondal, S., Ghosh, P., & Chakravorty, A. (1997). A Family of α -Amino Acid Salicylaldehydes Incorporating the Binuclear $\text{V}_2\text{O}_3^{3+}$ Core: Electrosynthesis, Structure, and Metal Valence. *Inorganic Chemistry*, **36**(1), 59-63.
- 2 Soghomonian, V., Chen, Q., Haushalter, R. C., Zubieta, J., & O'Connor, C. J. (1993). An inorganic double helix: hydrothermal synthesis, structure, and magnetism of chiral $[(\text{CH}_3)_2\text{NH}_2] \text{K}_4$

- [V10O10 (H₂O)₂ (OH)₄ (PO₄)₇] · 4H₂O. *Science*, 259(5101), 1596-1599.
- 3 Chen, Q., & Zubieta, J. (1993). Polyoxovanadium—Organophosphonates—Properties and Structure of an Unusual Pentavanadate Species with a V—O Group Directed Toward the Interior of the Molecular Cavity. *Angewandte Chemie International Edition in English*, **32**(2), 261-263.
- 4 Goc, A. (2006). Biological activity of vanadium compounds. *Central European Journal of Biology*, **1**, 314-332.
- 5 Boyd, D. W., & Kustin, K. E. N. E. T. H. (1984). Vanadium: a versatile biochemical effector with an elusive biological function.
- 6 Posner, B. I., Shaver, A., & Fantus, I. G. (1990). Insulin mimetic agents: vanadium and peroxovanadium compounds. *New antidiabetic drugs*, 107-118
- 7 Stern, A., Yin, X., Tsang, S. S., Davison, A., & Moon, J. (1993). Vanadium as a modulator of cellular regulatory cascades and oncogene expression. *Biochemistry and cell biology*, **71**(3-4), 103-112
- 8 Elgrishi, N., Rountree, K. J., McCarthy, B. D., Rountree, E. S., Eisenhart, T. T., & Dempsey, J. L. (2018). A practical beginner's guide to cyclic voltammetry. *Journal of chemical education*, **95**(2), 197-206.
- 9 Bard, A. J., Faulkner, L. R., & White, H. S. (2022). *Electrochemical methods: fundamentals and applications*. John Wiley & Sons.
- 10 Nageeb, A. S., Morsi, M. A., Gomaa, E. A., Hammouda, M. M., & Zaky, R. R. (2023). Comparison on Biological Inspection, Optimization, Cyclic Voltammetry, and Molecular Docking Evaluation of Novel Bivalent Transition Metal Chelates of Schiff Base Pincer Ligand. *Journal of Molecular Structure*, 137281.
- 11 Hussein, S. Q., El-Defrawy, M. M., Gomaa, E. A., & El-Ghalban, M. G. (2023). Analytical electrochemical sensing of calcium ions in HCl media in the presence of a dithizone ligand with its biological applications. *International*

- Journal of Electrochemical Science*, **18(9)**, 100249
- 12 Sultan, M. S., El-Defrawy, M. M., & Gomaa, E. A. (2022). Electrochemical Reduction Reaction of Potassium Chromate with Orange G and Giemsa Stain Dyes in HCl Solution Using Cyclic Voltammetry and Quantum Chemistry Properties. *Egyptian Journal of Chemistry*.
 - 13 Khan, A., Ahmed, R., & Mirza, M. (2010). Evaluation of kinetic parameters of uranyl acetate complexes in ethanolic solution by cyclic voltammetry. *Journal of Radioanalytical and Nuclear chemistry*, **283(2)**, 527-531.
 - 14 Gomaa, E. A. (2012). Solubility and solvation parameters of barium sulphate in mixed ethanol-water mixtures at 301.15 K. *International Journal of Materials and Chemistry*, **2(1)**, 16-18.
 - 15 García-Miranda Ferrari, A., Foster, C. W., Kelly, P. J., Brownson, D. A., & Banks, C. E. (2018). Determination of the electrochemical area of screen-printed electrochemical sensing platforms. *Biosensors*, **8(2)**, 53.
 - 16 Bamford, C.H., Compton, R.G., Thomas, J.D.R. (1986) *Electrode kinetics: Principles and Methodology* (Comprehensive Chemical Kinetics, Elsevier, Amsterdam, vol. 26(ISBN 0-4 4 4-42550-0).
 - 17 El-Shereafy, S. E., Gomaa, E. A., Yousif, A. M., & Abou Elyazed, A. (2017). Electrochemical and thermodynamic estimations of the interaction parameters for bulk and nano-silver nitrate (NSN) with cefdinir drug using a glassy carbon electrode. *Iranian Journal of Materials Science and Engineering*, **14(4)**, 48-57.
 - 18 Zhao, K., Song, H., Zhuang, S., Dai, L., He, P., & Fang, Y. (2007). Determination of nitrite with the electrocatalytic property to the oxidation of nitrite on thionine modified aligned carbon nanotubes. *Electrochemistry Communications*, **9(1)**, 65-70.
 - 19 Brownson, D. A., Banks, C. E., Brownson, D. A., & Banks, C. E. (2014). Interpreting electrochemistry. The handbook of graphene electrochemistry, 23-77.
 - 20 Shaikh, A. A., Begum, M., Khan, A. H., & Ehsan, M. Q. (2006). Cyclic voltammetric studies of the redox behavior of iron (III)-vitamin B 6 complex at carbon paste electrode. *Russian Journal of Electrochemistry*, **42**, 620-625.
 - 21 Gomaa, E. A., Negm, A., & Tahoon, M. A. K. (2016). Study of redox behavior of Cu (II) and interaction of Cu (II) with lysine in the aqueous medium using cyclic voltammetry. *European Journal of Chemistry*, **7(3)**, 341-346.
 - 22 Gomaa, E. A., Negm, A., & Tahoon, M. A. K. (2016). Study of redox behavior of Cu (II) and interaction of Cu (II) with lysine in the aqueous medium using cyclic voltammetry. *European Journal of Chemistry*, **7(3)**, 341-346.
 - 23 Nicholson, R. S., & Shain, I. (1964). Theory of stationary electrode polarography. Single scan and cyclic methods applied to reversible, irreversible, and kinetic systems. *Analytical chemistry*, **36(4)**, 706-723.
 - 24 Gomaa, E. A., El-Defrawy, M. M., & Hussien, S. Q. (2020). Estimation of cyclic voltammetry data for SrCl₂, CaCl₂ and their interaction with ceftriaxone sodium salt in KNO₃ using palladium working electrode. *European Journal of Advanced Chemistry Research*, **1(5)**.
 - 25 Abd El-Hady, M. N., Gomaa, E. A., & Al-Harazie, A. G. (2019). Cyclic voltammetry of bulk and nano CdCl₂ with ceftazidime drug and some DFT calculations. *Journal of Molecular Liquids*, **276**, 970-985.